Transition from continuous to discontinuous material failure in a simple model of an adhesive layer

M. Ferer
Department of Physics, West Virginia University, P.O. Box 6315, Morgantown, West Virginia 26506-6315

Duane H. Smith
U.S. Department of Energy, Federal Energy Technology Center, Morgantown, West Virginia 26507-0880
and Department of Physics, West Virginia University, Morgantown, West Virginia 26506-6315

(Received 9 June 1998)

A fine-scale, quasistatic model was used to study the removal of a disordered adhesive layer by a uniform force applied perpendicular to the layer. The model includes randomly chosen bonding forces of adhesion between imaginary ''gridblocks'' within the layer and a substrate, as well as cooperative forces of cohesion between adjacent gridblocks. For small cooperative forces, the amount of failure varies continuously with the applied force F. From infinitesimal failure at a minimum threshold value of the force, the fraction of the layer removed, $f_m(F)$, increases to encompass the total layer, as the applied force increases. This layer-removal function sharpens as the cooperative forces are increased; i.e., the slope of the layer-removal function, $\Delta f_m/\Delta F$, increases, so that the amount of failure is more and more sensitive to changes in the applied force. Indeed, this slope diverges with an exponent $\gamma \approx 0.85$ when the cooperative forces are approximately 2.1 as large as the adhesive forces. At small values of the cooperative forces, the layer-removal initiates at many locations and spreads to nearby blocks. The perimeter enclosing the area removed is fractal with a dimension $D_p \approx 1.3$. Increasing the cooperative forces causes the failure to initiate at fewer locations in the array, but to spread farther because of the larger cooperative forces. At the critical value of 2.1 for the ratio of cohesive to adhesive forces, the number density of these initiation sites goes to zero, and the ''correlation'' length (average range of the spread of failure) diverges with exponent $\nu \approx 0.5$. The characteristic time required for failure also diverges at the same critical value of cohesive/adhesive ratio with an exponent, $\Delta \approx 0.9$. Therefore, increasing the cooperative forces of cohesion effects a transition from the continuous response reminiscent of systems with depinning transitions to the discontinuous response characteristic of standard material fracture. Indeed, the divergent correlation length signals a transition to the long-range elastic forces that have enabled mean-field (fiber-bundle) models to be used in the study of standard material fracture. [S1063-651X(98)07012-3]

PACS number(s): 81.40.Np, 62.20.Mk, 02.70.Ns, 61.43.Bn

I. INTRODUCTION

Material failure is an issue of major importance and has, therefore, been widely studied for well over a century. Much of this work has naturally focused on the buildup of stress at defects, the formation of cracks, the energy changes during the process, and the dynamics of the crack propagation [1–21]. A number of quasimicroscopic or microscopic models have been used to study these important questions [6–12,22,23]. Recently, it has been appreciated that the long range of the elastic interactions permits a mean-field treatment of ordinary fracturing [18], which treatment can be mapped onto the democratic fiber-bundle model [14–17].

Although similar in spirit to much of this quasimicroscopic modeling, our model has two distinct material strengths: an adhesive strength, which tries to maintain contact of the layer with the substrate, and a cohesive strength, which tries to maintain the integrity of the layer. The separation of these two effects in the model enables the independent study of various features of material failure, which are less easily disentangled in the more traditional models. The applied stress causes failure at a threshold that scales primarily with the adhesive force. However, the cohesive forces introduce cooperative effects that lead to the familiar buildup of stress at defects; this both lowers and sharpens the failure threshold (i.e., lowers the stress at which layer removal occurs and decreases the range of stresses required to advance from infinitesimal to complete layer removal). For strong cohesive forces, we observed the familiar first-order-like behavior associated with a steplike threshold, as in fiber-bundle models, [14,24], where nearly total removal (i.e., failure) occurs above threshold but no failure occurs below threshold. In subsequent papers, we focused on the continuous failure in the model for small cohesive forces, discussing its similarities and its differences compared to depinning transitions and sandpile models [25]; in another paper, we focused on the size and shape of the fragments formed during the removal of the layer [26]. In this paper, we focus on the transition from continuous failure to discontinuous failure at a ''critical'' ratio of the strengths of the cohesive and adhesive forces.

In general, this model describes the strength of a layer adhering to a substrate in the presence of a uniform force that attempts to remove the layer. Although this model was motivated by problems encountered in the removal of the layer of filter cake from cylindrical filters (see Fig. 1) during the backpulse cleaning cycle of hot gas filtration for pressurized fluidized bed combustion [27–30], more mundane realizations include the flaking of paint off of a wall or the adhesion of tape. A similar model was used to study the electrical

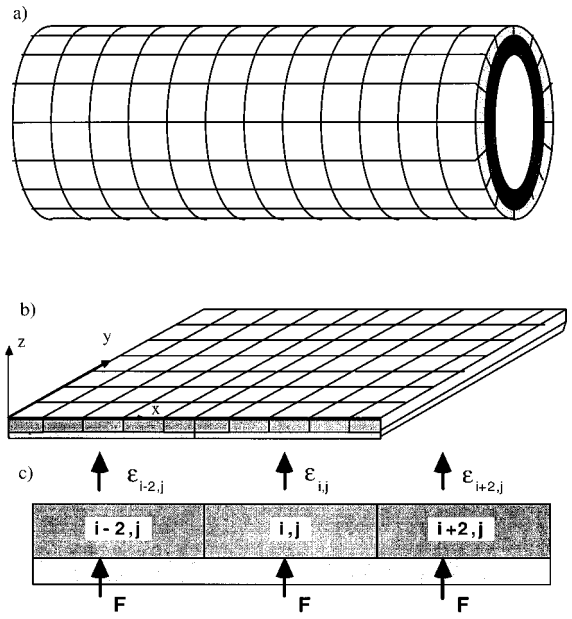

FIG. 1. (a) Cylindrical filter cake subdivided into blocks. (b) Simplified ''planar'' model with periodic boundary conditions connecting the $y=0$ and $y=200$ edges to mimic the cylindrical symmetry. (c) A small cross section showing forces and displacements.

conductivity of a layer; however, in that work, the layer remained on the substrate because the adhesive forces were very strong, making the ratio of cohesive to adhesive forces approximately zero, and fragmentation occurred within the layer because of lateral thermal expansion of the substrate [31].

In our model, increasing the strength of the cohesive forces effects a transition from continuous material failure, reminiscent of depinning transitions and sandpile models [32], to the discontinuous material failure, reminiscent of ordinary fracture and the fiber-bundle models [1,14–18]. In studying this transition from continuous to discontinuous material failure, we focus on (i) the layer-removal function (threshold in earlier papers, e.g., [24]), which we define to be the force dependence of the fraction of mass removed; (ii) the spatial characteristics of the regions of failure; and (iii) the characteristic time required for the material failure.

The layer-removal function is defined as the fractional mass (number of blocks) that is removed at a given value of applied force, i.e., $f_m(F)=\lim_{t\to\infty} m(F,t)/M_{\rm tot}$. For values of the cohesive forces below the transition, this layer removal, $f_m(F)$, is a continuous function [25] whose slope increases to infinity as one approaches the transition at a critical value of the ratio of cohesive to adhesive forces. For stronger cohesive forces (above the transition), the layer-removal function is steplike to within the accuracy of our finite-size simulations. In Sec. III, we characterize the dependence of this layer-removal function upon the cohesive to adhesive strength ratio. We find that the slope, df_m/dF, of the layer removal diverges at a critical value of this cohesive to adhesive ratio, while the position of the midpoint of the layer function, $F_{1/2}$, varies smoothly through this transition. The shape of these layer-removal functions and their sharpening with thickness are in qualitative agreement with experimental results for removal of dust cake from filters [33]; also the sharpening of the layer-removal function is consistent with the practical engineering observation that cleaning efficiency is poor if the cake is too thin and that efficiency improves with a thicker cake [34].

Figures 2 show the near-midpoint failure patterns for a given realization at a variety of cohesive strengths. As discussed in the next section, ''thickness factor,'' T is proportional to the cohesive strength, being the ratio of cohesive to adhesive strengths. For all cases in Fig. 2, failure starts at initiation sites (the darkest regions) and progresses to nearby sites (the gray scale lightens as time evolves); there is no failure in the white regions. An important consequence of the cohesive forces can be seen in these failure patterns. Increasing the cooperative forces (i) decreases the number of initiation sites and (ii) increases the range of failure. In Sec. IV, we present quantitative evidence that the number density of the initiation sites decreases to zero for an infinite system, while the range of the failure spreading out from these initiation sites diverges. In Sec. V, we show that the characteristic times required for failure diverge at the same critical value of the cohesive strength.

II. DESCRIPTION OF THE FINE-SCALE MODEL

In the physical system motivating this model, a layer of filter cake is deposited on a cylindrical candle filter to some thickness t; then a backpulse of compressed air is applied from the inside of the candle filter to blow the filter cake off, cleaning the filter. The force actually responsible for removing the layer of filter cake is due to the pressure drop P across the layer. Details specific to the filter cake removal function have been discussed in Refs. [24–26]. In this section, we present a simplified version of the model.

In our model, the layer is gridded into rectangular blocks. Our model system [shown in Fig. 1(b)] is assumed to be flat, lying in the x-y plane; however, continuity around the cylinder is preserved by periodic boundary conditions in the y direction. The layer-removal force F is applied, perpendicular to the layer, at the base of each block; as a result each block will be displaced by some small amount ε, in the z direction. This applied force will be balanced by the adhesive and cohesive spring forces (with spring constants k^a and k^c, respectively). Equation (1) presents the basic relation between the applied force F on a block at $r=\frac{1}{2}(i,j)$ and (i and j are even integers determining the location along the x and y directions, respectively) and the displacements of that block and the surrounding blocks:

$$F=k^a_{i,j}\varepsilon_{i,j}-\{k^c_{i-1,j}(\varepsilon_{i-2,j}-\varepsilon_{i,j})+k^c_{i+1,j}(\varepsilon_{i+2,j}-\varepsilon_{i,j}) +k^c_{i,j-1}(\varepsilon_{i,j-2}-\varepsilon_{i,j})+k^c_{i,j+1}(\varepsilon_{i,j+2}-\varepsilon_{i,j})\}. \quad (1)$$

Here each k^a is the spring constant of the adhesive spring between the (i,j) block and the substrate, and each k^c is the spring constant of the cohesive spring between two adjacent blocks. The model is defined so that the average stiffness of the adhesive springs is one-half, and the average stiffness of the cohesive springs is $T/2$ (i.e., $\langle k^a\rangle=\frac{1}{2}$ and $\langle k^c\rangle=T/2$). This parameter T, which we have called the thickness parameter, gives the ratio of average cohesive to average adhesive force. As discussed in Refs. [24–26], this thickness param-

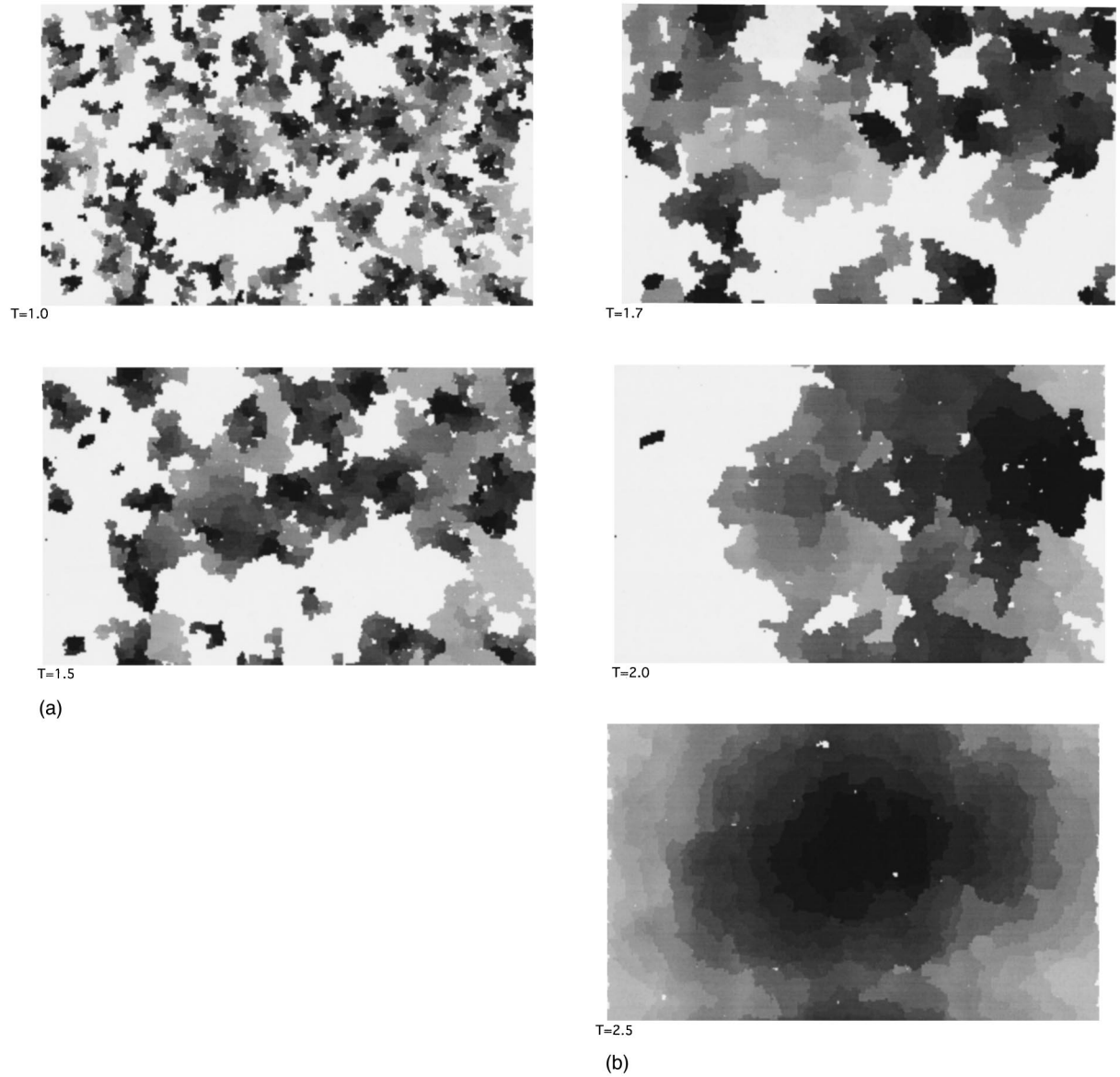

FIG. 2. Failure patterns for 64k systems with thicknesses $T=1.0$, 1.5, 1.7, 2.0, and 2.5. The mass was removed first in the darkest region and last in the lightest gray region. Mass still adheres to the substrate in the white regions. These show the effect of increasing cohesive forces on decreasing the number of failure initiation sites (sites of early time failure) and in increasing the growth of the regions of failure. Except for the change in thickness, the realizations are identical (i.e., same sets of random numbers, relatively weak bonds in the same locations, etc.).

eter depends upon the thickness of the filter cake layer, which is sensible since the cohesive strength of a layer should depend upon the thickness of that layer. Equation (1) may now be solved for the displacement of any one block (i,j), $\varepsilon_{i,j}$. Given the distributions of stiffnesses and the value of the force F, one guesses values of the displacements and then iterates this set of equations for all of the displacements $\varepsilon_{i,j}$ until the displacements stabilize between iterations. If any adhesive spring is stretched beyond its strength, S^a, i.e.,

$$k^a_{i,j}\varepsilon_{i,j} > S^a_{i,j}, \tag{2}$$

that spring will break. Similarly, if any cohesive spring is stretched beyond its strength, S^c, i.e.,

$$k^c_{i,j+1}|\varepsilon_{i,j}-\varepsilon_{i,j+2}| > S^c_{i,j+1}, \tag{3}$$

that cohesive spring will break. As with the spring constants, the strengths are chosen so that the average value of the strength of the adhesive springs is given by $\langle S^a\rangle=\frac{1}{2}$ and so that the average value of the strength of the cohesive springs is given by $\langle S^a\rangle=T/2$. This model is similar to many models of quasistatic, tensile fracturing in the scientific literature [6–12]. However, to our knowledge, this is the only modeling study of the material failure process in which the single-particle forces and two-particles force are clearly delineated in that their relative effect can be tuned through a parameter T.

It is natural to assume that the observed time dependence of the filter cake removal (on the order of a few milliseconds) [35] is much slower than the elastic relaxation of the layer of filter cake (e.g., the inverse frequency of elastic waves or the speed of sound—on the order of fractions of

milliseconds) [36,37]. This justifies a quasistatic process where the layer reaches elastic equilibrium [as given by Eq. (1)] between successive breaking of bonds; this quasistatic model seems especially justified near the threshold, where the failure occurs slowly, requiring many time steps. The computations in our quasistatic model proceed as follows: (i) with the layer, at equilibrium, under no load, the removal force F is applied; (ii) the layer reaches a new elastic equilibrium (the set of equations for the displacements is iterated until stabilization is reached); (iii) then at the end of this time step, each bond weaker than the actual stress is broken, Eqs. (2) and (3); (iv) steps (ii) and (iii), which together constitute one time step, are repeated, until a final time step at which no further bonds break. Once some bonds have broken at the end of a time step, the nearby bonds will be under a greater stress, increasing the likelihood that they will break at the end of the next time step. In this cascade, more bonds break than would have broken without the interaction mediated by the cohesive bonds. Thus the cooperative effect resulting from the cohesive bonds produces a cascade that lowers and sharpens the threshold, i.e., strengthening the cohesive bonds both decreases the removal force at which cleaning occurs and decreases the range of forces required to progress from infinitesimal to complete layer removal.

In reality, the ''cohesive'' forces may be even more significant than the ''adhesive'' forces. The ''thickness parameter'' T is the ratio of these two forces (also of the two breaking stresses), so that in Eqs. (1)–(3) varying T will vary the relative effect and importance of the adhesive and cohesive forces (and strengths). Therefore, the natural variables in our problem are (i) the applied removal force F; (ii) the thickness parameter T; (iii) the number of time steps; (iv) the system size, i.e., the number of blocks; as well as (v) the distributions of stiffnesses and strengths. To reduce the complexity of the results, we will assume that the applied removal force F is constant and uniform, but the model is not limited to this simplification. In all of our simulations, we have chosen a uniform distribution of stiffnesses. Each of the spring constants was chosen randomly from a flat distribution. However, relying on the spring analogy for the filter cake, we assume that thicker bonds between granules in the filter cake will be both stiffer and stronger since they can be mimicked by more springs connecting the granules; for this reason, each strength was strongly correlated with the stiffness, in that each strength was chosen randomly from a Gaussian distribution, which was sharply peaked about the value for that spring constant. Using a more sharply peaked distribution of stiffnesses and strengths would only serve to further sharpen this threshold, narrowing the range of removal forces over which the failure occurs; this would partially mask the effect we are investigating [24].

III. DIVERGENCE IN THE RESPONSE OF MASS REMOVAL TO APPLIED FORCE

Figure 3 shows the mass $m(F,t)$ (i.e., number of blocks) removed as a function of applied force F and time t for thickness $T=1.5$, where the cohesive forces are one and a half times as large as the adhesive forces for several values of the removal force. For large enough forces, all of the mass (here, $m_{\rm tot}=64k$) will be removed; while for small forces, no

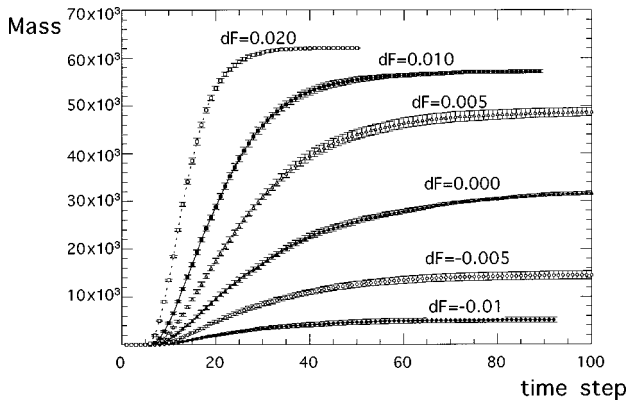

FIG. 3. Mass removed vs time for $64k$ models with thickness $T=1.5$ at forces $F=F_{1/2}+dF$ from $dF=-0.010$ to $dF=0.020$. $F_{1/2}=0.2578\pm0.0003$. Each datum represents the average of $m(t,F)$ over ten different realizations for the same time and the same value of dF (difference between the applied force and the midpoint force for each of the realizations).

mass is removed. In all cases, there is a short preremoval period (weakly force dependent) where bonds are breaking but no mass is removed. Then, mass is removed at a force-dependent rate up to a limiting fractional value, $f_m(F)=\lim_{t\to\infty} m(F,t)/m_{\rm tot}$ beyond which no more mass is removed or bonds broken. The transition from continuous to discontinuous behavior is most clearly shown in this force dependence of the limiting fractional mass removal. This layer-removal function $f_m(F)$ (threshold function in earlier papers, e.g., Ref. [24]) is shown in Fig. 4 for $T=1.5$. This threshold function is best characterized by the midpoint location where half of the mass is removed, $F_{1/2}$, and by the maximum slope, $\chi=(df_m/dF)_{\rm max}$ (slope at the inflection point, which occurs near the midpoint).

Thus far, all of the data presented are for systems with 64 000 blocks that are 320 blocks long and 200 blocks ''around the filter.'' We have performed numerous simulations for systems with sizes from 875 to 64×10^3 blocks. Figure 5 shows the values for $F_{1/2}$ and $\chi=(df_m/dF)_{\rm max}$ for

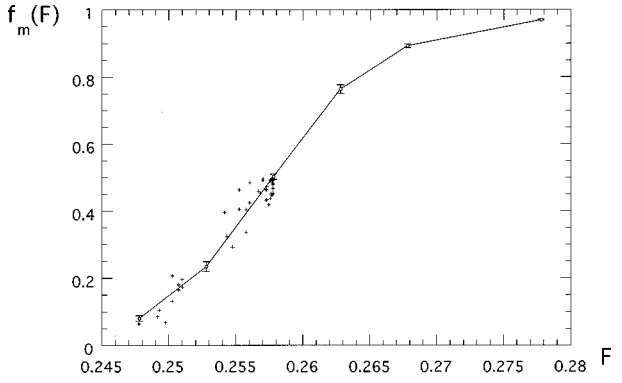

FIG. 4. Layer-removal function vs applied force for thickness $T=1.5$ fractional mass removed $f_m(F)=M(\infty,F)/M_{\rm tot}$ vs applied force F, where $M_{\rm tot}=64k$. The open circles give the $t=\infty$ results from Fig. 3. The + symbols give results from individual realizations from the runs used to determine $F_{1/2}$ for each realization; in this figure, these data were shifted horizontally so that the midpoint force for each realization was at 0.2578, which is the average value of the midpoint force.

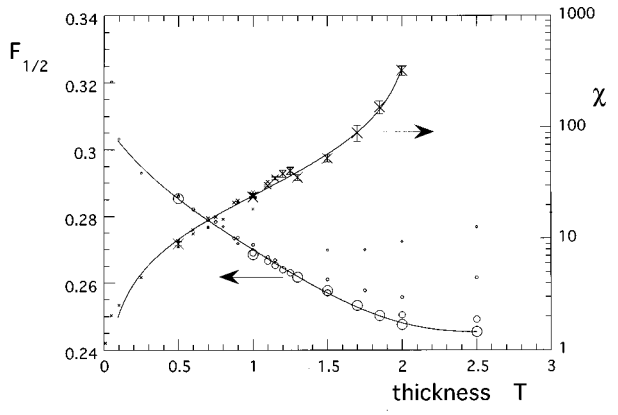

FIG. 5. The response of the layer removal to applied force, i.e., $\chi=(df_m/dF)_{\max}$ (x, right vertical axis) and the value of the force required for removal of one-half of the mass, i.e., $F_{1/2}$ (open circles, left vertical axis) plotted vs thickness for a variety of system sizes from 875 blocks (the smallest symbols), $4k$, $16k$, and lastly $64k$ (the largest symbols). The solid lines show the fits discussed in the text.

a variety of thicknesses as well as a variety of system sizes; the standard errors that are smaller than the plot symbols are not shown. The solid lines show the data fits discussed below. These data suggest a second-to first-order transition at a thickness between $2.0<T<2.5$. The data for $\chi=(df_m/dF)_{\max}$ in this figure show that any divergence must occur for $T>2$. Data from $64k$ systems for $T=2.5$ show a discontinuous layer-removal function with 94.8% removal at threshold and 0.006% removal for a force 0.001 below threshold; this determines an upper bound of $T=2.5$ on the location of the transition.

Because of fluctuations near the transition, finite-size effects cause the data to become very noisy and essentially uninterpretable near the transition; however, the data seem interpretable and, therefore, hopefully, reliable (i) up to $T\approx 0.9$ for the 875-block systems, (ii) up to $T\approx 1.2$ for the $4k$ systems, (iii) up to $T\approx 1.3$ for the $16k$ systems, and (iv) up to $T\approx 2$ for the $64k$ systems. All of the results presented are from simulations for these ranges where the data are only moderately noisy and seem accessible to reliable interpretation. Furthermore, the results presented have a negligible size dependence in the above ranges; however, above the transition, there is evidence of the usual decrease in strength with increasing system size [1].

While the data for $\chi=(df_m/dF)_{\max}$ and $f_m(F)$ are consistent with a transition of some sort for $2<T<2.5$, the data for $F_{1/2}$ are unaffected by this transition, decreasing smoothly through the transition; a simple polynomial fit to the data for $F_{1/2}$ is shown in Fig. 5 [38]. The apparent divergence in $\chi=(df_m/dF)_{\max}$ is well represented by a power-law fit as shown in Figs. 5 and 6,

$$\chi=(df_m/dF)_{\max}=A\left(\frac{T_c}{T}-1\right)^{-\gamma}, \tag{4}$$

where $A=26.4\pm 1.0$, $\gamma=0.85\pm 0.03$, and $T_c=2.10\pm 0.02$, with an $R=0.993$, which indicates that the transition occurs at $T_c\approx 2.1$. The standard error in the fitting of the critical

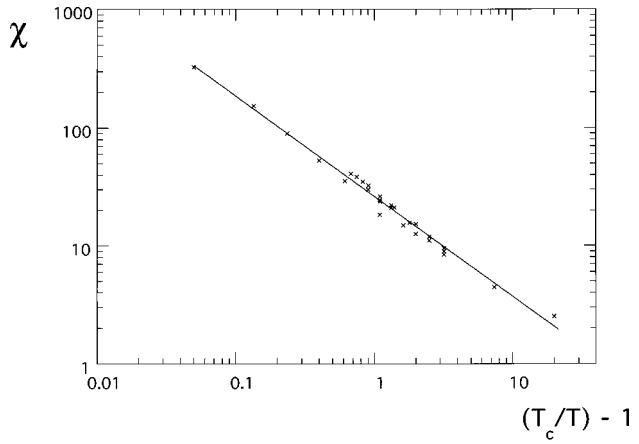

FIG. 6. Log-log plot of $\chi(T)=(df_m/dF)_{\max}$ vs $\{(T_c/T)-1\}$. The solid line shows the power-law fit to the data [Eq. (4)].

value of the strength ratio seems optimistic given all the possible sources for error; we believe that a more conservative value is a more reliable estimate of the real uncertainty, i.e., $T_c=2.1^{+0.2}_{-0.1}$.

Figure 7 illustrates how well the data for $f_m(F)$ are characterized by these fits to $\chi=(df_m/dF)_{\max}$ and $F_{1/2}$ in Fig. 6. In Fig. 7, these fits are used in an attempt to collapse the data for the fractional layer-removal function from $T=0.5$ up to $T=2.0$ for the two largest system sizes. All of the fractional layer-removal functions have a form similar to the $T=1.5$ case in Fig. 4. The fit to $F_{1/2}$ [38] shifts the midpoints of the layer-removal functions horizontally so that all occur at zero variable; the fit to the maximum slope, Eq. (4), spreads the range of the horizontal variable so that all the near-midpoint slopes in Fig. 7 have the value 1 in terms of the new variable. The success of this collapse supports our focusing upon the parametrization of the threshold function using midpoint and slope. This success also argues that the threshold function can be described by a single universal function, where all of the thickness dependence only serves to scale the applied force variable.

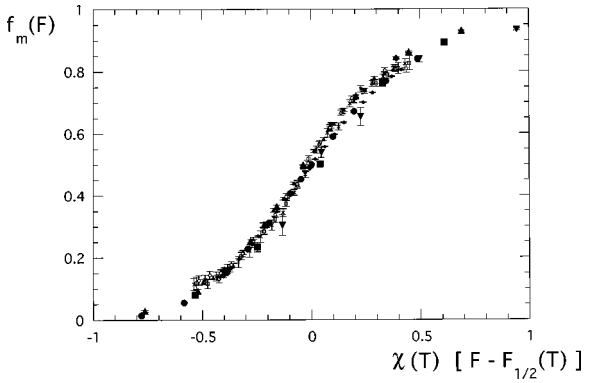

FIG. 7. The fits in Fig. 5 [i.e., $\chi(T)$ and $F_{1/2}(T)$] are used to collapse data for $f_m(F)$ for both $64k$ (large symbols) and $16k$ (small symbols) data for thicknesses $T=0.5$, 1, 1.15, 1.2, 1.25, 1.3, 1.5, and 1.7. This shows how successfully the two fits collapse the threshold function $f_m(F)$ to a single scaling function of the variable $\chi(T)$ $[F-F_{1/2}(T)]$, which shifts the midpoint and adjusts the slope.

IV. CHARACTERIZING THE CLEANING PATTERNS

The effect that increased cohesive strength has upon the cleaning patterns is illustrated by Fig. 2. Increasing the strength of the cohesive forces both decreases the number of sites at which failure initiates and increases the eventual spread of the failure, until at $T=2.5$ the failure initiates at one site and spreads throughout the array.

From these patterns, it also seems clear that the regions of failure are compact with a rough boundary. In an earlier paper [25] we found that the area was indeed compact and that the fractal dimension of the length of the perimeter enclosing the cleaned regime was $D_p=1.30\pm0.05$ for $T=0.5$ and 1.0, using a variety of system sizes. Fractal analyses of the perimeter for the simulations under consideration here are consistent with this value of the fractal dimension for all thicknesses up to the transition.

We have defined a quantity similar to correlation length in an attempt to quantify the observed (see Fig. 2) decrease in the number of sites at which failure initiates and the observed increase in the range of the spread of failure as the thickness parameter is increased to its value at the transition. This ''correlation'' length is defined as the root-mean-square (rms) radius of independently initiating clusters, which are, in turn, defined using the following rule. In determining whether a new failure regime was correlated with previous failure, a somewhat arbitrary cutoff distance of 2.3α was employed, where α is the lattice spacing, i.e., the distance between two adjacent blocks. At any given time step in the quasistatic process, if localized failure occurs in a regime that is further than 2.3α from any sites in an existing cluster, this is interpreted as a new initiation site starting a new cluster; if the localized failure is closer than 2.3α to an existing cluster, this new failure belongs to that existing cluster. The distance of 2.3α was chosen because several instances were observed where a block this close to a large cluster was removed; and the removal of such a block clearly was correlated to the large cluster. More distant correlated removals were not observed.

The number of these independent clusters is the number of failure initiation sites, which we observed to decrease with increasing thickness: see Fig. 2. To estimate the size of the cluster, the rms radius of each cluster is then determined; these rms radii are then averaged over all the clusters in the realization and then over all realizations.

Clearly, these definitions are not perfect: if failure occurs in a region near to, but further than 2.3α from, a region of previous failure, the new failure will be treated as a new failure initiation site even though it may be correlated with the earlier, nearby failure. Therefore, for larger cohesive forces, the number of initiation sites for thicker systems may be overestimated, since failure more distant than 2.3 lattice spacings may be correlated to earlier failure. Also, for smaller cohesive forces, the number of initiation sites may be underestimated, since two regions of failure closer than 2.3 lattice spacings may be uncorrelated. In any case, this prescription provides a quantitative estimate of the number of independent initiation sites and the subsequent size of the clusters that grow from these initiation sites. Lacking a rigorous procedure for determining correlation length ξ as one has in thermodynamic phase transitions, this, or some equally flawed alternative, may be the best estimate of the correlation length.

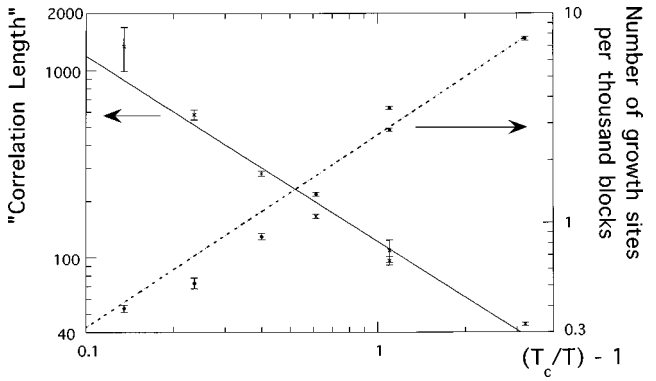

FIG. 8. Log-log plot of the correlation length (x, solid line—left-hand vertical axis) and the number density of initiation sites (solid circles, dashed line—right-hand vertical axis) vs $\{(T_c/T)-1\}$ for both $64k$ and $16k$ block systems. The lines show the power law fits, Eqs. (5) and (6).

The results for the number of initiation sites and average cluster size are given in Fig. 8. The number of initiation sites $n(T)$ goes to zero, with a near-linear dependence (slope 1 on the log-log plot), as the strength of the cohesive forces approach their critical value,

$$n(T)\approx B\left(\frac{T_c}{T}-1\right)^{\lambda}, \tag{5}$$

where $B=2.6\pm0.2$ and $\lambda=0.92\pm0.07$, with an $R=0.99$. The power-law fit to the divergence in the square of the correlation length closely matches the divergence in the response of the failure to changes in the applied force, Eq. (4); i.e.,

$$\xi^2=e^2\left(\frac{T_c}{T}-1\right)^{-2\nu}, \tag{6}$$

where $e^2=122\pm6$ and $2\nu=0.99\pm0.04$, with an $R=0.99$. In these fits, we assume $T_c=2.1$.

Of course, the nonrigorous definition of correlation length is a concern. However, as stated above, for the stronger cohesive forces, we expect that this correlation length will overestimate the number of initiation sites and underestimate the correlation length. Therefore, if this definition errs, it errs by making $n(T)$ larger than it should be and ξ^2 smaller than it should be, so that, if anything, $n(T)$ might go to zero faster and ξ^2 might diverge faster than shown in Fig. 8. This only strengthens the quantitative evidence for a divergent correlation length. These long-range correlations at and above the transition are just the long-range interactions in standard elastic systems, which validate the use of mean-field theory or fiber-bundle models for studying standard fracture [14,18].

V. DIVERGENCE OF THE CHARACTERISTIC TIME AT THE CRITICAL POINT

Not surprisingly, the onset of the instability that we have been studying is associated with a divergence in the time required for the process. Fortunately, it is simpler to develop

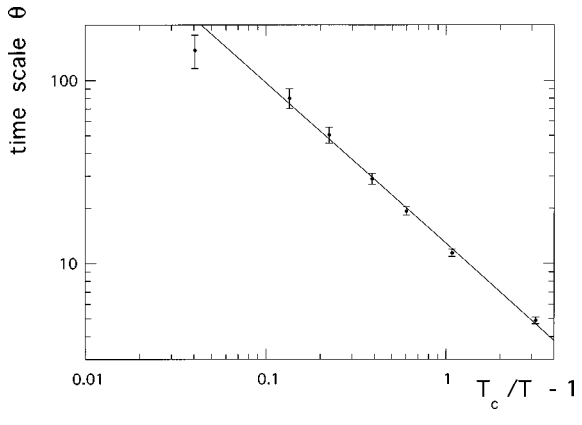

FIG. 9. The characteristic time $\theta(T)$ vs $[(T_c/T-1)]$, Eq. (10); the straight line shows a power-law fit to the data, Eq. (7).

a reliable definition of characteristic time than it was a definition for the correlation length. We choose to define a time associated with the midrange of the threshold function (e.g., $dF=0$ in Fig. 3), because this midrange seems to be so robust, in that size dependence ([25], also Figs. 5 and 7) and even variations between different realizations [25] are unimportant here. At a removal force equal to $F_{1/2}$, where half of the mass will eventually be removed, we define the characteristic time θ to be that time at which one quarter of the total mass is removed, i.e., the midpoint mass for this applied force, $m(F_{1/2},\theta)=\frac{1}{2}m(F_{1/2},\infty)$ (e.g., $m=16k$ and $\theta\equiv t\approx 27$ for $dF=0$ in Fig. 3). At this time $t=\theta$, $m(F_{1/2},t)$ is changing the most rapidly, so that there will be less error in determining this time than there would be for a time where the mass were varying slowly. Figure 9 shows the graph of this characteristic time plotted versus $[(T_c/T)-1]$, where again, we use the critical value of cohesive forces from our fit of $\chi=(df_m/dF)_{\max}$ in Figs. 5 and 6, $T_c=2.1$. The divergence in this characteristic time is well represented by the power law

$$\theta=A_t\left(\frac{T_c}{T}-1\right)^{-\Delta}, \tag{7}$$

where $A_t=12.83\pm 0.35$ and $\Delta=0.88\pm 0.03$, with an $R=0.998$. Again a value of the exponent similar to that for the force response of the failure in Eq. (4) and to that for the correlation length in Eq. (6) is obtained.

VI. CONCLUSIONS

In our simple model of the removal of an adhesive layer, we have located and characterized a transition from continuous to discontinuous dependence of the dynamical response upon the driving force. In the regime of continuous dependence of the dynamical response, the behavior is not unlike the behavior for depinning transitions or sandpile models, where the system has no response below a minimum value of the driving force (depinning threshold), and where the response increases uniformly from zero as the force increases above this minimum value. However, in an earlier paper, we found that quantitative comparison with depinning transitions was problematic, perhaps because of the cohesive forces [25].

For strong enough cohesive forces, the response is discontinuous, in that there is no dynamical response infinitesimally below a threshold value of the applied force, while infinitesimally above this threshold value a significant fraction of the layer is removed. This is similar to the behavior of fractures in a material under tensile stress, in that at a threshold value of the stress a macrocrack occurs, which will spread from one side of the sample to the other at this constant value of the stress. Because these elastic forces are so long range (the stress field will decrease as $1/\sqrt{r}$ from the edge of the crack [1]) fracturing can be studied using mean-field theory, which is known to be valid if the interactions are long range, and which is equivalent to the more traditional fiber-bundle model [14–18]. Our model provides an opportunity for studying the onset of this long-range, elastic interaction at the transition.

We have presented evidence that a transition from continuous to discontinuous layer removal occurs at a critical value of the ratio of cohesive to adhesive forces. This ratio is approximately 2.1. Although such quantitative details may not be correctly predicted for an infinite system because of the notoriously subtle size dependence of material failure [1,12,25], the evidence supporting the qualitative behavior near the transition is convincing for finite systems. *This transition occurs when the strength of the two-particle forces is enhanced by increasing the thickness parameter to a critical value at which the qualitative nature of the failure changes.* This approach to a critical value of the thickness appears to be associated with a power-law divergence of (i) the response of layer removal to changes in the applied force, (ii) a rather crudely defined correlation length, and (iii) a characteristic time for the removal. This behavior is extremely reminiscent of the thermodynamic behavior near second-order critical points, where *a transition occurs when the effect of two-particle forces (energy/kT) is enhanced by a temperature reduction to a critical temperature at which the system begins to phase separate*. This approach to the critical temperature is also associated with power-law divergences in (i) the response of the order parameter to ordering field (e.g., the response of volume V to pressure P, i.e., dV/dP near vapor-liquid transitions; the response of magnetization M to magnetic field H, i.e., dM/dH for ferromagnetic transitions; etc.), (ii) the correlation length, and (iii) the relaxation time [39–41]. We have allowed the apparent similarity between the dynamical critical point of our model and the thermodynamics of critical points to influence our definitions of the power laws, Eqs. (4), (6), and (7).

ACKNOWLEDGMENT

We gratefully acknowledge the support of the U.S. Department of Energy, Office of Fossil Energy.

[1] V. Z. Parton, *Fracture Mechanics: From Theory to Practice* (Gordon and Breach, Philadelphia, 1992).
[2] A. A. Griffith, Philos. Trans. R. Soc. London, Ser. A **221**, 163 (1920).
[3] B. Cotterell and J. R. Rice, Int. J. Fract. **16**, 155 (1980).
[4] A. Munjiza, D. R. J. Owen, and N. Bicanic, Eng. Comput. **12**, 145 (1995).
[5] W. Fenghui, Z. Xuilin, and L. Mingxu, Int. J. Fract. **70**, R19 (1995).
[6] H. J. Hermann and S. Roux, *Statistical Models for the Fracture of Disordered Media* (North-Holland, Amsterdam, 1990).
[7] P. Meakin, Science **252**, 226 (1991).
[8] Y. Termonia and P. Meakin, Nature (London) **320**, 429 (1986).
[9] E. Louis and F. Guinea, Europhys. Lett. **3**, 871 (1987).
[10] H. Furukawa, Phys. Rev. E **52**, 5124 (1995).
[11] H. J. Hermann, A. Hansen, and S. Roux, Phys. Rev. B **39**, 637 (1989).
[12] L. de Arcangelis, S. Redner, and H. J. Hermann, J. Phys. (France) Lett. **46**, 1585 (1985); P. M. Duxbury, P. L. Leath, and P. D. Beale, Phys. Rev. B **36**, 367 (1987).
[13] E. S. C. Ching, J. S. Langer, and H. Nakanishi, Phys. Rev. Lett. **76**, 1087 (1996).
[14] H. E. Daniels, Proc. R. Soc. London, Ser. A **183**, 405 (1945).
[15] P. C. Hemmer and A. Hansen, J. Appl. Mech. **59**, 909 (1992).
[16] D. Sornette, J. Phys. A **22**, L243 (1989).
[17] D. J. Sornette, J. Phys. I **2**, 2089 (1992).
[18] S. Zapperi, P. Ray, H. E. Stanley, and A. Vespignani, Phys. Rev. Lett. **78**, 1408 (1997).
[19] F. Barpi and S. Valente, in *Cohesive Crack Model*, edited by M. Guiggiani, Proceedings of AIMETA '97, the 13th Biennial Conference of the Italian Association of Theoretical and Applied Mechanics in Siena, Italy, September 29–October 3, 1997 (Edizioni ETS, Pisa, Italy, 1997), Vol. 3, pp. 55–60.
[20] I. Monetto, in *Analysis of Plates with Interacting Cracks*, Proceedings of AIMETA '97, the 13th Biennial Conference of the Italian Association of Theoretical and Applied Mechanics in Siena, Italy, September 29–October 3, 1997 (Edizioni ETS, Pisa, Italy), Vol. 3, pp. 85–90.
[21] P. Bocca, A. Carpinteri, and S. Valente, Int. J. Solids Struct. **27**, 1139 (1991).
[22] L. Golubovic, A. Peredera, and M. Golubovic, Phys. Rev. E **52**, 4640 (1995).
[23] L. Golubovic and A. Peredera, Phys. Rev. E **51**, 2799 (1995).
[24] M. Ferer and D. H. Smith, J. Appl. Phys. **81**, 1737 (1997); M. Ferer, M. C. Petcu, G. Parsamian, and Duane H. Smith, in *A Simple Model of the Adhesive Failure of a Layer–Cohesive Forces & Fractal Nature of the Failure*, edited by M. Guiggiani, Proceedings of AIMETA '97, the 13th Biennial Conference of the Italian Association of Theoretical and Applied Mechanics in Siena, Italy, September 29–October 3, 1997 (Edizioni ETS, Pisa, Italy, 1997), Vol. 1, p. 19.
[25] M. Ferer and D. H. Smith, Phys. Rev. E **57**, 866 (1998).
[26] M. Ferer and D. H. Smith, Aerosol. Sci. Technol. **29**, 246 (1998).
[27] J. M. Weeldon, in *Experimental Results from the Grimethorpe PFBC Facility*, Proceedings of the Eighth International Conference of Fluidized Bed Combustion (U.S.D.O.E./M.E.T.C., Morgantown, West Virginia, 1985), Vol. 1, pp. 317–335.
[28] M. J. Mudd and J. D. Hoffman, in *Tidd PFBC Hot Gas Filter Operating Experiences: July 1993–April 1994*, Proceedings of the 1994 Conference on Coal Fired Power Systems (U.S.D.O.E./M.E.T.C., Morgantown, West Virginia, 1994), pp. 520–534.
[29] T. E. Lippert, G. J. Bruck, and J. Isakksson, in *Karhula Hot Gas Cleanup Results*, Proceedings of the 1994 Conference on Coal Fired Power Systems (U.S.D.O.E./M.E.T.C., Morgantown, West Virginia, 1994), pp. 535–544.
[30] T. E. Lippert, R. A. Newby, M. A. Alvin, D. M. Bachovchin, and E. E. Smeltzer, in *PFBC Dust Cake Studies*, Proceedings of the 1994 Conference on Coal Fired Power Systems (U.S.D.O.E./M.E.T.C., Morgantown, West Virginia, 1994), pp. 580–590.
[31] K. M. Crosby and R. M. Bradley, Phys. Rev. E **55**, 6084 (1997).
[32] F. Family and T. Vicsek, *Dynamics of Fractal Surfaces* (World Scientific, Singapore, 1991); P. Bak, C. Tang, and K. Wiesenfeld, Phys. Rev. A **38**, 364 (1988).
[33] E. Schmidt, Chem. Eng. Technol. **21**, 26 (1998); J. Sievert, and F. Loeffler, Filtr. Sep. **24**, 424 (1987).
[34] Paul M. Eggerstedt (private communication).
[35] S. Laux, B. Giernoth, H. Bulak, and U. Renz, *Proceeding of the 12th International Conference on Fluidized Bed Combustion*, San Diego, California, May 9–13, edited by X. Rubow (ASME, New York, 1993).
[36] J. S. Langer and H. Nakanishi, Phys. Rev. E **48**, 439 (1993).
[37] F. Abraham, D. Brodbeck, R. Rafey, and W. Rudge, Phys. Rev. Lett. **73**, 272 (1994).
[38] The fifth-order polynomial that is used to fit the data for $F_{1/2}$ in Fig. 5 and that is used to collapse the data in Fig. 7 is given by $F_{1/2}=0.3084-0.0644T+0.05241T^2-0.03884T^3+0.01436T^4-0.00188T^5$.
[39] M. E. Fisher, Rep. Prog. Phys. **30**, 615 (1967).
[40] L. P. Kadanoff *et al.*, Rev. Mod. Phys. **39**, 395 (1967).
[41] H. E. Stanley, *Introduction to Phase Transitions and Critical Phenomena* (Oxford University Press, New York, 1971).